

Cite this: *Dalton Trans.*, 2024, **53**, 6496Received 8th March 2024,  
Accepted 25th March 2024

DOI: 10.1039/d4dt00702f

rsc.li/dalton

Catalytic dinitrogen reduction to hydrazine and ammonia using  $\text{Cr}(\text{N}_2)_2(\text{diphosphine})_2$  complexes†Charles H. Beasley,<sup>a</sup> Olivia L. Duletski,<sup>a</sup> Ksenia S. Stankevich,<sup>a</sup> Navamoney Arulsamy,<sup>b</sup> and Michael T. Mock<sup>\*a</sup>

The synthesis, characterization of *trans*- $[\text{Cr}(\text{N}_2)_2(\text{depe})_2]$  (**1**) is described. **1** and *trans*- $[\text{Cr}(\text{N}_2)_2(\text{dmpe})_2]$  (**2**) catalyze the reduction of  $\text{N}_2$  to  $\text{N}_2\text{H}_4$  and  $\text{NH}_3$  in THF using  $\text{SmI}_2$  and  $\text{H}_2\text{O}$  or ethylene glycol as proton sources. **2** produces the highest total fixed N for a molecular Cr catalyst to date.

Motivated by the desire to understand and control the challenging multi-proton, multi-electron reaction of  $\text{N}_2$  reduction to  $\text{NH}_3$ , researchers have intensely studied the reactivity of molecular transition metal dinitrogen complexes.<sup>1</sup> Well-defined molecular systems offer a high degree of electronic and structural control to regulate chemical reactivity of  $\text{N}_2$ .<sup>2</sup> When combined with effective strategies to form N–H bonds, such as proton-coupled electron transfer (PCET) reagents,<sup>3</sup> *i.e.*  $\text{SmI}_2$  and a proton source, tens-of-thousands of equivalents of  $\text{NH}_3$  can be generated.<sup>4</sup> The valuable information obtained from these studies includes the identification of viable M– $\text{N}_2\text{H}_y$  reaction intermediates from spectroscopic data that can be used to delineate the mechanistic steps of a putative catalytic cycle. Such studies can aid in the understanding of the mechanistically complex biological  $\text{N}_2$  fixation processes carried out by nitrogenase enzymes,<sup>5</sup> as well as heterogeneous Haber–Bosch catalysts.<sup>6</sup>

Group 6  $\text{N}_2$  complexes bearing monodentate phosphine ligands, especially with Mo and W, were among the first molecular systems to generate stoichiometric quantities of  $\text{N}_2$ -derived  $\text{NH}_3$  from protonolysis reactions with strong acids nearly 50 years ago.<sup>7</sup> Recently, a renaissance of examining structurally similar  $[\text{M}(\text{N}_2)_2(\text{P–P})_2]$ , (M = Mo, W; P–P = diphosphine) systems has begun, elevating these simple complexes as catalysts for  $\text{N}_2$  reduction to  $\text{NH}_3$ , or other remarkable reac-

tions such as cleavage of the  $\text{N}_2$  triple bond.<sup>8</sup> Masuda and co-workers reported spontaneous  $\text{N}\equiv\text{N}$  bond cleavage upon one-electron oxidation of *trans*- $[\text{Mo}(\text{N}_2)_2(\text{depe})_2]$  (depe =  $\text{Et}_2\text{PCH}_2\text{CH}_2\text{PEt}_2$ ) to form  $[\text{Mo}(\text{N})(\text{depe})_2]^+$ .<sup>9</sup> Chirik and co-workers developed a photocatalytic strategy to form  $\text{NH}_3$  from  $[\text{Mo}(\text{N})(\text{depe})_2]^+$  and  $\text{H}_2$ .<sup>10</sup> Electrocatalytic  $\text{N}_2$  fixation with Mo and W-phosphine complexes was described by Peters and co-workers using a tandem catalysis approach.<sup>11</sup> Nishibayashi and co-workers showed simple Mo-phosphine complexes catalyzed  $\text{N}_2$  reduction to  $\text{NH}_3$  using  $\text{SmI}_2$  and various proton sources.<sup>12</sup>

While these examples highlight new discoveries using  $[\text{M}(\text{N}_2)_2(\text{P–P})_2]$  (M = Mo, W) complexes, catalytic  $\text{N}_2$  reduction with analogous Cr compounds are limited. Recent reports highlighted the utility of molecular Cr complexes using a variety of ligand architectures for  $\text{N}_2$  activation,<sup>8a,13</sup> functionalization,<sup>14</sup> or catalytic  $\text{N}_2$  silylation.<sup>15</sup> However, molecular Cr complexes that catalyze the direct reduction of  $\text{N}_2$  to  $\text{NH}_3$  are rare. In 2022, Nishibayashi and co-workers reported a Cr complex bearing a PCP pincer ligand that catalyzed direct  $\text{N}_2$  reduction to  $\text{NH}_3$  and  $\text{N}_2\text{H}_4$  at  $-78^\circ\text{C}$  to rt.  $\text{KC}_8$  and phosphonium salts as  $\text{H}^+$  sources were required for turnover, and this system was not catalytic using  $\text{SmI}_2$ .<sup>16</sup> Herein we prepared and characterized *trans*- $[\text{Cr}(\text{N}_2)_2(\text{depe})_2]$  (**1**), and report catalytic  $\text{N}_2$  reduction to  $\text{NH}_3$  and  $\text{N}_2\text{H}_4$  with **1** and *trans*- $[\text{Cr}(\text{N}_2)_2(\text{dmpe})_2]$ <sup>17</sup> (**2**) (dmpe =  $\text{Me}_2\text{PCH}_2\text{CH}_2\text{PMe}_2$ ) at room temperature using  $\text{SmI}_2$  and ethylene glycol or  $\text{H}_2\text{O}$  as proton sources.

Vigorous stirring of yellow *trans*- $[\text{CrCl}_2(\text{depe})_2]$ <sup>18</sup> (**1-Cl**) in THF with excess Mg powder under a  $\text{N}_2$  atmosphere for 24 h furnished **1** as a dark red solid in 70% yield. Isolation of **1** allowed for a comparison of the structural and spectroscopic data with **2** that was reported in 1983.<sup>17a</sup> The structure of **1**, determined by single crystal X-ray diffraction, shows Cr with four phosphorus atoms of the chelates on the equatorial plane and two axial end-on bound  $\text{N}_2$  ligands, Fig. 1, panel a. The average Cr–N, Cr–P, and  $\text{N}\equiv\text{N}$  bond distances are  $1.904 \pm 0.005$  Å,  $2.334 \pm 0.007$  Å, and  $1.104 \pm 0.004$  Å, respectively. The corresponding Cr–N, and Cr–P, bond distances in **2** (see ESI†),

<sup>a</sup>Department of Chemistry and Biochemistry, Montana State University, Bozeman, MT 59717, USA. E-mail: michael.mock@montana.edu

<sup>b</sup>Department of Chemistry, University of Wyoming, Laramie, WY, 82071, USA

†Electronic supplementary information (ESI) available: Experimental procedures, crystallographic details, and additional spectroscopic and electrochemical data. CCDC 2330754 (**1**) and 2330755 (**2**). For ESI and crystallographic data in CIF or other electronic format see DOI: <https://doi.org/10.1039/d4dt00702f>

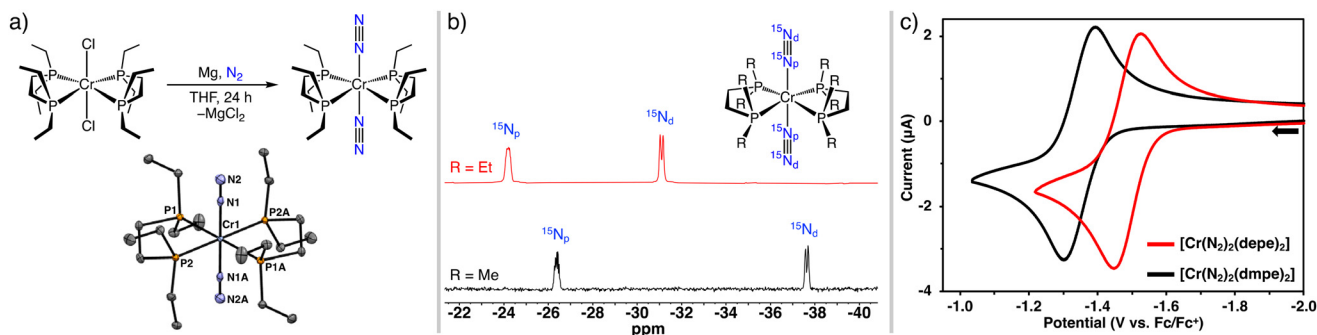


**Fig. 1** (a) Synthesis and molecular structure of **1**. Thermal ellipsoids are drawn at 50% probability. Hydrogen atoms are omitted for clarity. Crystals of **1** contain two molecules per asymmetric unit with comparable metric parameters; only one molecule is shown. Selected bond distances (Å) and angles (°): Cr1–N1 = 1.9081(10); N1–N2 = 1.1003(14); Cr–P1 = 2.3343(3); Cr–P2 = 2.3249(3). Cr2–N3 = 1.9008(10); N3–N4 = 1.1069(14); Cr–P3 = 2.3425(3); Cr–P4 = 2.3346(3). P1–Cr1–P2 = 81.650(9); P3–Cr2–P4 = 81.583(10); P1–Cr1–N1 = 89.25(3); P2–Cr1–N1 = 90.21(3); P3–Cr2–N3 = 89.29(3); P4–Cr2–N3 = 90.59(3). (b)  $^{15}\text{N}\{^1\text{H}\}$  NMR spectra of  $^{15}\text{N}$  (red) and  $^{215}\text{N}$  (black) recorded at 25 °C in THF- $d_8$ . (c) Cyclic voltammograms of **1** and **2** in THF showing the Cr $^{I/O}$  wave.

are slightly shorter at 1.8862(17) Å, and  $2.294 \pm 0.005$  Å, and the N≡N distance is 1.110(2) Å.<sup>19</sup> The ligand bite angles for **1** and **2**, *i.e.* P1–Cr–P2, are 81.6° and 83.5°, respectively, and the P–Cr–N angles are near 90°.

The  $^{31}\text{P}\{^1\text{H}\}$  NMR spectrum of **1** in THF- $d_8$ , displays a singlet at 79.9 ppm (68.8 ppm for **2**) consistent with four magnetically equivalent P atoms. Complexes **1** and **2** were characterized by  $^{15}\text{N}$  NMR spectroscopy to augment the cumulative library of tabulated  $^{15}\text{N}$  NMR data of phosphine-supported group 6  $\text{N}_2$  complexes.<sup>13h</sup> The  $^{15}\text{N}_2$ -labelled complexes  $^{15}\text{N}$  and  $^{215}\text{N}$ , were prepared by mixing the respective Cr– $\text{N}_2$  complexes in THF- $d_8$  under 1 atm  $^{15}\text{N}_2$ . The  $^{15}\text{N}$  NMR spectra were collected after mixing for 24 h. The  $^{15}\text{N}\{^1\text{H}\}$  NMR spectra contain two resonances; a doublet ( $J_{\text{NN}} = 7.0$  Hz) and a multiplet ( $\sim 2.5$  Hz  $^{31}\text{P}$  coupling) ( $^{15}\text{N}$ : –31.1 ppm, –24.2 ppm, and  $^{215}\text{N}$ : –37.6 ppm, –26.4 ppm), assigned as the distal ( $\text{N}_d$ ) and proximal ( $\text{N}_p$ ) nitrogen atoms, respectively, (Fig. 1, panel b).<sup>13i</sup>

Cyclic voltammetry (CV) experiments established the redox behaviour of the Cr(0)– $\text{N}_2$  complexes. Voltammograms were recorded using a glassy carbon working electrode at 0.1 V s $^{-1}$  in THF. The voltammogram for each complex displays a reversible, one-electron Cr $^{I/O}$  wave with the half-wave potential ( $E_{1/2}$ ) of –1.49 V and –1.34 V (*vs.* Cp $_2$ Fe $^{+/0}$ ) for **1** and **2**, respectively (Fig. 1, panel c). The electrochemically reversible Cr $^{I/O}$  couples indicate  $\text{N}_2$  dissociation does not occur upon oxidation to Cr(I) during the CV experiments. The reversibility of the waves for **1** and **2** contrasts other *cis*- or *trans*-[Cr( $\text{N}_2$ ) $_2$ (P $_4$ )] complexes measured by CV that exhibit quasi-reversible or irreversible Cr $^{I/O}$  waves due to rapid  $\text{N}_2$  loss upon oxidation.<sup>13b,c,i</sup> In the current study, an irreversible anodic wave was assigned to the Cr $^{II/I}$  redox feature at  $E_{\text{pa}} = -0.48$  V and  $E_{\text{pa}} = -0.63$  V, for **1** and **2**, respectively, due to  $\text{N}_2$  dissociation at more positive potentials, (Fig. S17 and S18 ESI $^\dagger$ ). The CV results suggest a one-electron chemical oxidation to form *trans*-[Cr( $\text{N}_2$ ) $_2$ (P–P) $_2$ ] $^+$  should be possible; however, our attempts to isolate such a species have been unsuccessful. Owing to the more electron-rich metal centre of **1**, the  $\nu_{\text{NN}}$  band in the infrared spectrum

at 1906 cm $^{-1}$  (THF) appears at lower energy than the  $\nu_{\text{NN}}$  band for **2** at 1917 cm $^{-1}$  (THF).

Complexes **1** and **2** were examined as catalysts for the direct reduction of  $\text{N}_2$  to  $\text{NH}_3$  and  $\text{N}_2\text{H}_4$ . The catalysis studies were performed in THF at room temperature using the PCET reagent SmI $_2$  and ethylene glycol and/or water as proton donors. A typical catalytic run used 583 equiv. SmI $_2$ , 1166 equiv. ROH per Cr centre and was stirred for 48 h. Quantification of  $\text{NH}_3$ ,  $\text{N}_2\text{H}_4$  and  $\text{H}_2$  (see ESI for details $^\dagger$ ) products assessed the total fixed N generated in each reaction. Selected catalytic data are listed in Table 1 (see ESI for all tabulated results $^\dagger$ ).

Analysis of the catalysis results provides insights about the performance of **1** and **2** under identical reaction conditions. **2** afforded more total fixed N than **1** in all catalytic trials. For example, **1** generated up to 5 equiv. of  $\text{NH}_3$  and 5 equiv.  $\text{N}_2\text{H}_4$  per Cr center using ethylene glycol as the proton donor after >100 h. Under identical conditions, **2** produced up to 16 equiv.  $\text{NH}_3$  and 10 equiv.  $\text{N}_2\text{H}_4$  in 48 h. Furthermore, ethylene glycol worked more effectively as the proton donor affording higher total fixed N than using  $\text{H}_2\text{O}$ . The deleterious effect of  $\text{H}_2\text{O}$  on catalysis was noted in reactions with **2** using ethylene glycol as the primary proton source. As the amount of  $\text{H}_2\text{O}$  added to the reaction increased,  $\text{NH}_3$  production declined, while the  $\text{N}_2\text{H}_4$  formed stayed relatively constant. We postulate the Cr complexes may simply be more prone to degradation in the presence of  $\text{H}_2\text{O}$ . Separately, **2** was treated with 500 equiv.  $\text{H}_2\text{O}$  or ethylene glycol in THF- $d_8$ . Free dmpe from complex degradation appeared more rapidly using  $\text{H}_2\text{O}$ , as assessed by  $^{31}\text{P}$  NMR spectroscopy. Catalysis performed with **2** under an atmosphere of  $^{15}\text{N}_2$  afforded  $^{15}\text{NH}_4^+$  as a doublet at 7.1 ppm ( $J_{^{15}\text{N}-^1\text{H}} = 71$  Hz) in the  $^1\text{H}$  NMR spectrum, identifying  $^{15}\text{N}_2$  as the source of  $^{15}\text{NH}_3$ .

Catalytic trials using *trans*-[CrCl $_2$ (dmpe) $_2$ ] (**2-Cl**) and ethylene glycol generated comparable amounts of  $\text{NH}_3$  and  $\text{N}_2\text{H}_4$  as using **2** as the precatalyst. **1-Cl** did not catalyze  $\text{N}_2$  reduction, affording only 1 equiv. of  $\text{NH}_3$  and  $\text{N}_2\text{H}_4$  per Cr center. SmI $_2$

**Table 1** Selected Cr-catalyzed N<sub>2</sub> reduction experiments
$$\text{N}_2 + \text{SmI}_2 + \text{ROH} \xrightarrow[\text{THF, rt}]{[\text{Cr}] \text{ cat.}} \text{NH}_3 + \text{N}_2\text{H}_4 + \text{H}_2$$

Entry	Cr cat.	ROH	NH <sub>3</sub> equiv./Cr <sup>a</sup>	N <sub>2</sub> H <sub>4</sub> equiv./Cr <sup>b</sup>	Total fixed N	Time (h)
1	None	(CH <sub>2</sub> OH) <sub>2</sub>	0	0	0	48
2	<b>1</b>	(CH <sub>2</sub> OH) <sub>2</sub>	3.7 ± 0.9	1.4 ± 0.8	4.9 <sup>h</sup> ± 1.5	48
3	<b>1</b>	(CH <sub>2</sub> OH) <sub>2</sub>	4.6 ± 0.6	4.0 ± 1.7	8.6 <sup>h</sup> ± 2.1	100
4 <sup>c</sup>	<b>1</b>	H <sub>2</sub> O	1.4	0.7	2.1	48
5 <sup>d</sup>	<b>1</b>	H <sub>2</sub> O	3.2	0.6	3.8	28
6	<b>1-Cl</b>	(CH <sub>2</sub> OH) <sub>2</sub>	1.2	0.9	2.1	48
7	<b>2</b>	(CH <sub>2</sub> OH) <sub>2</sub>	14.6 ± 1.6	5.9 ± 2.9	20.5 <sup>h</sup> ± 3.8	48
8 <sup>e</sup>	<b>2</b>	(CH <sub>2</sub> OH) <sub>2</sub>	6.2 ± 0.5	6.4 ± 0.8	12.6 <sup>h</sup> ± 0.3	48
9 <sup>f</sup>	<b>2</b>	(CH <sub>2</sub> OH) <sub>2</sub>	4.4 ± 0.9	6.6 ± 0.6	11 <sup>h</sup> ± 0.4	48
10 <sup>g</sup>	<b>2</b>	(CH <sub>2</sub> OH) <sub>2</sub>	1.1	5.7	6.8	48
11 <sup>d</sup>	<b>2</b>	H <sub>2</sub> O	5.1	5.9	11	3
12	<b>2-Cl</b>	(CH <sub>2</sub> OH) <sub>2</sub>	13.5 ± 2.8	5.9 ± 0.6	19.4 <sup>h</sup> ± 3.4	48

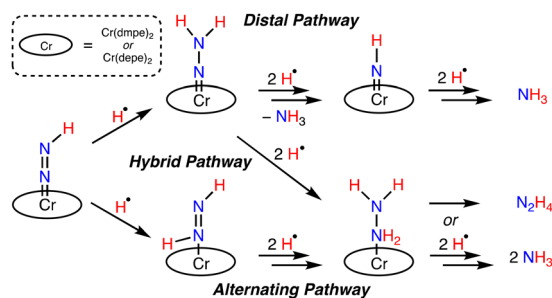
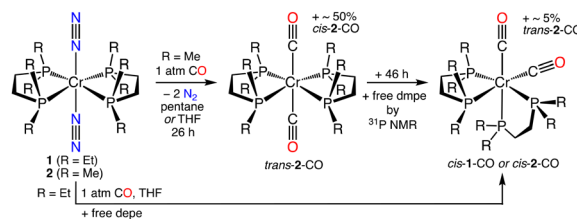
Experiments performed using 0.6 μmol catalyst in 15.0 mL THF at 25 °C under 1 atm N<sub>2</sub>, with 583 equiv. of SmI<sub>2</sub>, and with 1166 equiv. ROH unless otherwise specified. <sup>a</sup> Determined by acidification and NH<sub>4</sub><sup>+</sup> quantification using <sup>1</sup>H NMR spectroscopy (see ESI<sup>†</sup>). <sup>b</sup> Determined by colorimetric *p*-dimethylaminobenzaldehyde method (see ESI<sup>†</sup>). <sup>c</sup> 1000 equiv. H<sub>2</sub>O/Cr. <sup>d</sup> 10 000 equiv. H<sub>2</sub>O/Cr. <sup>e</sup> 25 ppm of H<sub>2</sub>O. <sup>f</sup> 250 ppm of H<sub>2</sub>O. <sup>g</sup> 583 equiv. (CH<sub>2</sub>OH)<sub>2</sub>, 583 equiv. H<sub>2</sub>O. <sup>h</sup> Average of two or more trials. H<sub>2</sub> quantification by gas chromatography, values are tabulated in ESI<sup>†</sup>.

and ethylene glycol may be ineffective at reducing the Cr(II) center of **1-Cl** to Cr(0) where N<sub>2</sub> is strongly activated. Treatment of **2-Cl** with 2 equiv. SmI<sub>2</sub> and 2 equiv. ethylene glycol rapidly generated **2** (see ESI<sup>†</sup>). However, the same reaction of **1-Cl** and SmI<sub>2</sub> with ethylene glycol additive did not form **1** (*E*<sub>1/2</sub> = -1.49 V, *vide supra*). **1** or **2** could not be generated from **1-Cl** or **2-Cl** using excess SmI<sub>2</sub>(THF) alone (*E*<sup>o</sup> of SmI<sub>2</sub>(THF) = -1.41 ± 0.08 V<sup>20</sup> vs. Fc/Fc<sup>+</sup>). A Cr(I) species could be accessible, but N<sub>2</sub> activation and subsequent functionalization steps may be moderated at Cr(I), limiting catalysis.

The mixed N<sub>2</sub> reduction selectivity to form NH<sub>3</sub> and N<sub>2</sub>H<sub>4</sub> provides preliminary evidence for a catalytic cycle that follows, at least in part, an alternating N<sub>2</sub> reduction mechanism, Fig. 2, bottom. A purely distal N<sub>2</sub> reduction pathway, Fig. 2, top, would be selective for NH<sub>3</sub> formation. In a 1986 report, the reaction of **2** with CF<sub>3</sub>SO<sub>3</sub>H was postulated to form a Cr-hydrazido product, [Cr(NNH<sub>2</sub>)(dmpe)<sub>2</sub>][CF<sub>3</sub>SO<sub>3</sub>]<sub>2</sub>.<sup>21</sup> A recent study by Wei, Yi, Xi, and co-workers examining early stage N<sub>2</sub> functionalization of [Cp\*Cr<sup>0</sup>(depe)(N<sub>2</sub>)]<sup>-</sup> (Cp\* = η<sup>5</sup>-C<sub>5</sub>(CH<sub>3</sub>)<sub>5</sub>) using a variety of electrophiles (H<sup>+</sup>, Me<sub>3</sub>Si<sup>+</sup>, Me<sup>+</sup>) also revealed the selective formation of Cr-hydrazido products, consistent

with a distal pathway. Contrary to these reaction patterns, protonation studies of related *cis*- or *trans*-[Cr(N<sub>2</sub>)<sub>2</sub>(P<sub>4</sub>)] complexes we examined using strong acids or H<sup>+</sup>/e<sup>-</sup> reagents, as well as the catalytic Cr[PCP] system<sup>16</sup> generated NH<sub>3</sub> and N<sub>2</sub>H<sub>4</sub>.<sup>13c,i,15a</sup> Considering all these examples, and that N<sub>2</sub> reduction mechanisms are sensitive to reaction conditions, (*i.e.* identity of the H<sup>+</sup> and e<sup>-</sup> reagents, solvent, temperature), a hybrid N<sub>2</sub> reduction pathway<sup>22</sup> where the third and fourth N-H bonds are formed at the proximal N atom of a Cr-hydrazido intermediate, Fig. 2, middle, cannot be excluded for the current systems. Further studies are warranted to understand the N<sub>2</sub> reduction pathways with Cr.

The proclivity for N<sub>2</sub> ligand substitution in **1** and **2** was evaluated as a metric that could reflect catalyst stability and influence catalytic performance. We examined reactions of **1** and **2** with CO to assess the rate of ligand exchange, Fig. 3. Ligand substitution in these six-coordinate complexes is expected to be a dissociative process; a result of Cr-N or Cr-P bond dissociation. Wilkinson, Hursthouse, and co-workers noted **2** did not react with 7 atm CO for several hours except under u.v. irradiation (in light petroleum) to form *cis*-[Cr(CO)<sub>2</sub>(dmpe)<sub>2</sub>] (*cis*-2-CO).<sup>17b</sup> This account was surprising, and the unreactive nature toward N<sub>2</sub>/CO exchange seemed uncharacteristic of a

**Fig. 2** Plausible N<sub>2</sub> reduction mechanisms for Cr mediated formation of hydrazine and ammonia.**Fig. 3** Ligand exchange reactions of **1** and **2** with CO display different reaction profiles.

complex with terminally bound N<sub>2</sub> ligands. We reacted **2** with 1 atm CO at 25 °C in pentane or THF without u.v. irradiation and monitored the reaction by *in situ* IR spectroscopy, or <sup>31</sup>P NMR spectroscopy (see ESI†). In both solvents the reaction was slow, but **2** was not unreactive. In THF, after 26 h ~85% of **2** converted to a ~1:1 mixture of *cis*-**2**-CO and *trans*-[Cr(CO)<sub>2</sub>(dmpe)<sub>2</sub>] (*trans*-**2**-CO). *trans*-**2**-CO converts to ~95% *cis*-**2**-CO (and ~5% free dmpe) after additional 46 h by <sup>31</sup>P NMR spectroscopy. In THF, **1** converts directly to *cis*-[Cr(CO)<sub>2</sub>(depe)<sub>2</sub>] *cis*-**1**-CO ( $\nu_{\text{CO}} = 1829, 1768 \text{ cm}^{-1}$ ) in ~3 h by *in situ* IR spectroscopy (see ESI†). The vastly different rates of N<sub>2</sub>/CO ligand exchange underscore the greater kinetic stability of **2** toward Cr–L dissociative processes that could ultimately curtail catalyst deactivation pathways (*i.e.* ligand loss) improving catalyst performance for N<sub>2</sub> reduction compared to **1**.

In conclusion, we present a contemporary advancement in the use of *trans*-[Cr(N<sub>2</sub>)<sub>2</sub>(P–P)<sub>2</sub>] complexes (**1** and **2**) for direct catalytic reduction of N<sub>2</sub> to form NH<sub>3</sub> and N<sub>2</sub>H<sub>4</sub> using the PCET reagent SmI<sub>2</sub> and H<sub>2</sub>O and/or ethylene glycol as proton donors. A new complex, *trans*-[Cr(N<sub>2</sub>)<sub>2</sub>(depe)<sub>2</sub>], was presented herein. Despite having similar electronic structures, we posit **2** is a better catalyst than **1** (using the presented conditions), due to a less negative Cr<sup>I/0</sup> redox couple and greater kinetic stability from Cr–L dissociative processes.

## Author contributions

C. Beasley, investigation, methodology, writing, editing; O. L. Duletski, investigation; K. S. Stankevich, investigation; N. Arulsamy, investigation, writing; M. T. Mock, conceptualization, methodology, supervision, writing, editing, funding acquisition.

## Conflicts of interest

There are no conflicts of interest to declare.

## Acknowledgements

The authors thank Dr. Bernhard Linden and Mathias Linden for LIFDI-MS analysis. This material is based upon work supported by the National Science Foundation (NSF) under Grant No. CHE-1956161 and CHE-2247748. Support for MSU's NMR Center has been provided by the NSF (Grant No. NSF-MRI: CHE-2018388 and DBI-1532078), the Murdock Charitable Trust Foundation (2015066:MNL), and MSU's office of the Vice President for Research and Economic Development. The authors gratefully acknowledge financial support for the X-ray diffractometer from the NSF (CHE-0619920) and a Institutional Development Award (IDeA) from the National Institute of General Medical Sciences of the National Institutes of Health (Grant # 2P20GM103432).

## References

- (a) Y. Tanabe and Y. Nishibayashi, *Chem. Soc. Rev.*, 2021, **50**, 5201–5242; (b) Y. Tanabe and Y. Nishibayashi, *Coord. Chem. Rev.*, 2022, **472**, 214783; (c) *Transition Metal–Dinitrogen Complexes: Preparation and Reactivity*, ed. Y. Nishibayashi, Wiley-VCH, Weinheim, 2019.
- M. J. Chalkley, M. W. Drover and J. C. Peters, *Chem. Rev.*, 2020, **120**, 5582–5636.
- (a) Y. Ashida, K. Arashiba, K. Nakajima and Y. Nishibayashi, *Nature*, 2019, **568**, 536–540; (b) N. G. Boekell and R. A. Flowers II, *Chem. Rev.*, 2022, **122**, 13447–13477; (c) E. A. Boyd and J. C. Peters, *J. Am. Chem. Soc.*, 2022, **144**, 21337–21346.
- Y. Ashida, T. Mizushima, K. Arashiba, A. Egi, H. Tanaka, K. Yoshizawa and Y. Nishibayashi, *Nat. Synth.*, 2023, **2**, 635–644.
- C. Van Stappen, L. Decamps, G. E. Cutsail III, R. Bjornsson, J. T. Henthorn, J. A. Birrell and S. DeBeer, *Chem. Rev.*, 2020, **120**, 5005–5081.
- C. M. Goodwin, P. Lömker, D. Degerman, B. Davies, M. Shipilin, F. Garcia-Martinez, S. Koroidov, J. Katja Mathiesen, R. Rameshan, G. L. S. Rodrigues, C. Schlueter, P. Amann and A. Nilsson, *Nature*, 2024, **625**, 282–286.
- J. Chatt, A. J. Pearman and R. L. Richards, *Nature*, 1975, **253**, 39–40.
- (a) F. A. Darani, G. P. A. Yap and K. H. Theopold, *Organometallics*, 2023, **42**, 1324–1330; (b) S. J. K. Forrest, B. Schlusshass, E. Y. Yuzik-Klimova and S. Schneider, *Chem. Rev.*, 2021, **121**, 6522–6587; (c) C. E. Laplaza and C. C. Cummins, *Science*, 1995, **268**, 861–863.
- A. Katayama, T. Ohta, Y. Wasada-Tsutsui, T. Inomata, T. Ozawa, T. Ogura and H. Masuda, *Angew. Chem., Int. Ed.*, 2019, **58**, 11279–11284.
- (a) S. Kim, Y. Park, J. Kim, T. P. Pabst and P. J. Chirik, *Nat. Synth.*, 2022, **1**, 297–303; (b) M. T. Mock, *Nat. Synth.*, 2022, **1**, 262–263.
- P. Garrido-Barros, J. Derosa, M. J. Chalkley and J. C. Peters, *Nature*, 2022, **609**, 71–76.
- Y. Ashida, K. Arashiba, H. Tanaka, A. Egi, K. Nakajima, K. Yoshizawa and Y. Nishibayashi, *Inorg. Chem.*, 2019, **58**, 8927–8932.
- (a) A. J. Kendall and M. T. Mock, *Eur. J. Inorg. Chem.*, 2020, 1358–1375; (b) M. T. Mock, S. Chen, R. Rousseau, M. J. O'Hagan, W. G. Dougherty, W. S. Kassel, D. L. DuBois and R. M. Bullock, *Chem. Commun.*, 2011, **47**, 12212–12214; (c) M. T. Mock, S. Chen, M. O'Hagan, R. Rousseau, W. G. Dougherty, W. S. Kassel and R. M. Bullock, *J. Am. Chem. Soc.*, 2013, **135**, 11493–11496; (d) M. Fritz, S. Demeshko, C. Würtele, M. Finger and S. Schneider, *Eur. J. Inorg. Chem.*, 2023, **26**, e202300011; (e) W. H. Monillas, G. P. A. Yap, L. A. MacAdams and K. H. Theopold, *J. Am. Chem. Soc.*, 2007, **129**, 8090–8091; (f) W. H. Monillas, G. P. A. Yap and K. H. Theopold, *Inorg. Chim. Acta*, 2011, **369**, 103–119; (g) X. Wang, Y. Wang, Y. Wu, G. X. Wang, J. Wei and Z. Xi, *Inorg. Chem.*, 2023, **62**,

- 18641–18648; (h) M. T. Mock, A. W. Pierpont, J. D. Egbert, M. O'Hagan, S. Chen, R. M. Bullock, W. G. Dougherty, W. S. Kassel and R. Rousseau, *Inorg. Chem.*, 2015, **54**, 4827–4839; (i) J. D. Egbert, M. O'Hagan, E. S. Wiedner, R. M. Bullock, N. A. Piro, W. S. Kassel and M. T. Mock, *Chem. Commun.*, 2016, **52**, 9343–9346; (j) I. Vidyaratne, J. Scott, S. Gambarotta and P. H. M. Budzelaar, *Inorg. Chem.*, 2007, **46**, 7040–7049.
- 14 (a) J. Yin, J. Li, G. X. Wang, Z. B. Yin, W. X. Zhang and Z. Xi, *J. Am. Chem. Soc.*, 2019, **141**, 4241–4247; (b) G. X. Wang, X. Wang, Y. Jiang, W. Chen, C. Shan, P. Zhang, J. Wei, S. Ye and Z. Xi, *J. Am. Chem. Soc.*, 2023, **145**, 9746–9754; (c) G. X. Wang, Z. B. Yin, J. Wei and Z. Xi, *Acc. Chem. Res.*, 2023, **56**, 3211–3222; (d) Z. B. Yin, B. Wu, G. X. Wang, J. Wei and Z. Xi, *J. Am. Chem. Soc.*, 2023, **145**, 7065–7070; (e) T. Shima, J. Yang, G. Luo, Y. Luo and Z. Hou, *J. Am. Chem. Soc.*, 2020, **142**, 9007–9016; (f) Y. Kokubo, K. Tsuzuki, H. Sugiura, S. Yomura, Y. Wasada-Tsutsui, T. Ozawa, S. Yanagisawa, M. Kubo, T. Takeyama, T. Yamaguchi, Y. Shimazaki, S. Kugimiya, H. Masuda and Y. Kajita, *Inorg. Chem.*, 2023, **62**, 5320–5333.
- 15 (a) A. J. Kendall, S. I. Johnson, R. M. Bullock and M. T. Mock, *J. Am. Chem. Soc.*, 2018, **140**, 2528–2536; (b) M. C. Eaton, B. J. Knight, V. J. Catalano and L. J. Murray, *Eur. J. Inorg. Chem.*, 2020, 1519–1524; (c) J. Li, J. Yin, G. X. Wang, Z. B. Yin, W. X. Zhang and Z. Xi, *Chem. Commun.*, 2019, **55**, 9641–9644.
- 16 Y. Ashida, A. Egi, K. Arashiba, H. Tanaka, T. Mitsumoto, S. Kuriyama, K. Yoshizawa and Y. Nishibayashi, *Chem. – Eur. J.*, 2022, **28**, e202200557.
- 17 (a) G. S. Girolami, J. E. Salt, G. Wilkinson, M. Thornton-Pett and M. B. Hursthouse, *J. Am. Chem. Soc.*, 1983, **105**, 5954–5956; (b) J. E. Salt, G. S. Girolami, G. Wilkinson, M. Motevalli, M. Thornton-Pett and M. B. Hursthouse, *J. Chem. Soc., Dalton Trans.*, 1985, 685–692.
- 18 D. M. Halepoto, D. G. L. Holt, L. F. Larkworthy, G. J. Leigh, D. C. Povey and G. W. Smith, *J. Chem. Soc., Chem. Commun.*, 1989, 1322–1323.
- 19 Structural metrics from XRD data of 2 collected here at 100 K. Data from ref. 17 at 295 K.
- 20 (a) M. L. Kuhlman and R. A. Flowers II, *Tetrahedron Lett.*, 2000, **41**, 8049–8052; (b) R. J. Enemærke, K. Daasbjerg and T. Skrydstrup, *Chem. Commun.*, 1999, 343–344.
- 21 J. E. Salt, G. Wilkinson, M. Motevalli and M. B. Hursthouse, *J. Chem. Soc., Dalton Trans.*, 1986, 1141–1154.
- 22 (a) J. Rittle and J. C. Peters, *J. Am. Chem. Soc.*, 2016, **138**, 4243–4248; (b) N. B. Thompson, P. H. Oyala, H. T. Dong, M. J. Chalkley, J. Zhao, E. E. Alp, M. Hu, N. Lehnert and J. C. Peters, *Inorg. Chem.*, 2019, **58**, 3535–3549.